Scientia Iranica A (2014) 21(5), 1480–1491

SCIENTIA IRANICA

Sharif University of Technology
Scientia Iranica
Transactions A: Civil Engineering
www.scientiairanica.com

Safety evaluation of shallow tunnel based on elastoplastic-viscoplastic analysis

M. Maleki* **and M. Mousivand**

Department of Civil Engineering, Bu-Ali Sina University, Hamedan, Iran.

Received 1 August 2012; received in revised form 15 August 2013; accepted 22 April 2014

KEYWORDS
Soft ground;
NATM;
Elastoplastic;
Viscoplastic;
Constitutive model;
FLAC 2D.

Abstract. Application of an elastoplastic-viscoplastic constitutive model for tunnel safety evaluation is presented in this paper. For achieving this purpose, the model parameters were identified through FLAC code at first for a section of Tehran Towheed tunnel by a back analysis process (as a case study). Next, with definition of two safety parameters related to short term (time-independent) and long term (time-dependent) behaviors, the safety of tunnel was assessed. For the short term behavior, which is related to excavation phase of tunnel, the elastoplastic part plays the essential role, so the safety parameter was defined based on hardening variable of constitutive model. But for the long term behavior, time-dependent deformation will be generated during time, thus evaluation of safety was done by comparison of current shear strain and a defined limit shear strain based on experimental data. The results of back analysis showed a good capacity of model in reproduction of tunnel behavior. Application of defined safety parameters on Towheed tunnel indicates that stability of tunnel is guaranteed during construction stages and long term situation.

1. Introduction

There are numerous studies in the literature in which elastoplasticity theory has been applied to describe the ground behavior due to tunnelling [1-14]. The precision of prediction depends essentially on quality of constitutive model implemented in the numerical code. On the other hand, the type (isotropic, kinematic or mixed) and mathematical form of hardening mechanism, flow rule (associated or non-associated) and elastic mechanism play important roles in the quality (accuracy) of numerical analyses results of tunnel problem. However, according to experimental observations in the majority of geomaterials, a large part of the engendered deformations due to tunnelling occurs during the time [15-18]. Therefore, it is more realistic to introduce the effect of time in the numerical analysis of tunnel.

Various constitutive models with different degrees of sophistication and different ranges of application have been proposed to describe the viscous behavior of ground material. Different theories employed for modeling viscous effects are viscoelasticity, elasto-viscoplasticity, viscoelasticity-viscoplasticity and elastoplasticity-viscoplasticity. The majority of these models are based on the elasto-viscoplasticity concept. Most of the elasto-viscoplastic models use either Perzyna's overstress theory [19] or non-stationary flow surface theory. The key assumption in connection with the models of overstress types is that viscous effects are negligible in the elastic domain. This means that all of the inelastic strains happen during the time and for a very rapid loading, very small inelastic strains occurs, and when stress state is within the static yield surface (the case of cyclic loading) no plastic strain occurs. The other remark concerning the elasto-viscoplastic based on overstress theory is that the

*. *Corresponding author. Tel.: +98 811 8257410; Fax: +98 811 8257400*
E-mail addresses: maleki@basu.ac.ir (M. Maleki); mohsenmousivand@gmail.com (M. Mousivand)

failure of material cannot be modeled. In plasticity, it is the condition of consistency that allows the failure of materials to be modeled. This condition is not satisfied in the classical viscoplasticity theory, where the stress state can lie out of static yield surface. In the elasto-viscoplastic model based on non-stationary flow surface theory, the parameter of time is directly introduced in the formulation. This can violate the general validity of constitutive model. The Adachi & Oka model, Dafalias model, and Katona model are certain examples for overstress models, whereas Sekiguchi model, Dragon and Mroz model, Nova model and the Matsui and Abe model are the examples for elasto-viscoplastic model based on non-stationary flow surface theory [20-26]. Oka proposed a cyclic elasto-viscoplastic model for clay using nonlinear kinematic hardening law [27]. Kim developed a viscoelastic-viscoplastic model based on kinematic hardening for modeling the rate effect in cyclic loading of clay [28]. Kaliakin & Dafalias have proposed an elastoplastic-viscoplastic bounding surface model for clay [29]. This model considers the coupled elastoplasticity-viscoplasticity, so inelastic strain can occur for stress states within the bounding surface.

In this approach, application of a simple elastoplastic-viscoplastic model that is implemented in FLAC code for safety evaluation of shallow tunnel is verified. The model has been developed from a basic elastoplastic model (CJS) by considering an additional viscous mechanism. This model is able to explain the time-dependent behavior of soils such as creep (primary and secondary), stress relaxation and strain rate effects. In addition, the existing problems in the classical elasto-viscoplastic models, related to the plasticity failure and the rapid loading, are solved in the used constitutive model.

For tunnel, like any other structures during the construction and life time phases, safe and effective operations should be ensured [30]. Safety factor of tunnel is an important parameter to control its stability in each stage of construction or in any time after completion of tunnel. Two typical criteria exist in technical literature; one is based on critical stress and the other is based upon critical deformation [31-33]. In the present work, for construction phase, the hardening parameter in elastoplastic part of constitutive model is compared with its maximum value in failure state that defines a stress safety factor. For the life time phase of tunnel, where time-dependent deformation is generated, a limit deformation corresponding to the material failure state is defined. These two definitions allowed us to evaluate safety of tunnel in different phases of construction and after construction.

The suggested methodology for safety evaluation of tunnel was employed on Towheed tunnel of Tehran as a case study. In the first step, regarding some existing field data, the calculation code was calibrated using back analysis process. Afterwards, instantaneous and long-term safeties of tunnel were studied.

2. Brief representation of constitutive model

The chosen constitutive model in this study is decomposed into two elastoplastic (basic model) and viscoplastic parts according to the work of Maleki [34]. The basic model is a simplified version of the CJS. The CJS model is an elastoplastic constitutive model that has been developed in the Ecole Centrale de Lyon [35-37]. Viscoplastic part has been based on general overstress theory of Perzyna. The response of model is therefore decomposed as:

$$\dot{\varepsilon}_{ij} = \dot{\varepsilon}^{e}_{ij} + \dot{\varepsilon}^{p}_{ij} + \dot{\varepsilon}^{vp}_{ij}. \tag{1}$$

Two first parts are concerned with the basic elastoplastic model and the last part is related to the viscoplastic mechanism.

2.1. Elastoplastic part (basic model)

The basic model, besides the elastic part, comprises two plastic mechanisms. One is isotropic and the other is deviatoric. The yield surface of the isotropic mechanism is a plane perpendicular to the hydrostatic axis in the stress space. Evolution of this surface is governed by an isotropic hardening law. For the deviatoric mechanism, the flow rule is non-associated and the yield surface is piloted by an isotropic hardening law. The essential equations of the model are briefly presented below. Presentation of model in detail is given elsewhere [36,37].

2.1.1. Elastic part

The elastic law has been given in the form:

$$\dot{\varepsilon}^{e}_{ij} = \frac{\dot{S}_{ij}}{2G} + \frac{\dot{I}_1}{9K}\delta_{ij}, \tag{2}$$

in which $\dot{\varepsilon}^{e}_{ij}$ is the increment of the elastic strain tensor, $\dot{S}_{ij}$ the increment of the deviatoric stress tensor ($\dot{S}_{ij} = \dot{\sigma}_{ij} - \frac{\dot{\sigma}_{kk}}{3}\delta_{ij}$), δ_{ij} the Kronecker symbol, and $\dot{I}_1 = \dot{\sigma}_{kk}$ while G and K are the elastic shear and bulk modulus, respectively. These two parameters are related to the first invariant of stress tensor as:

$$K = K^{e}_{0}\left(\frac{I_1}{3P_a}\right)^{n}, \tag{3}$$

$$G = G^{e}_{0}\left(\frac{I_1}{3P_a}\right)^{n}, \tag{4}$$

where G_0, K^{e}_{0} and n are the model parameters and P_a is the reference pressure equal to 100 kPa.

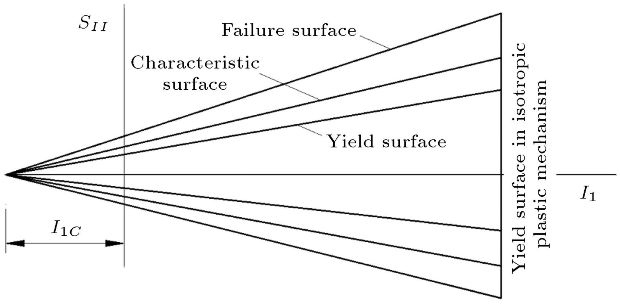

(a)

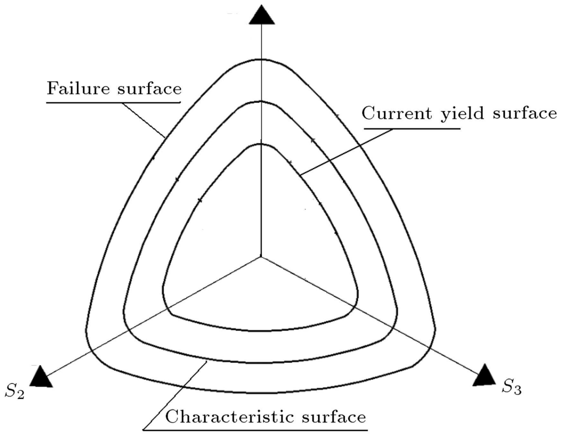

(b)

Figure 1. Presentation of the yield, failure, critical state, and characteristic surfaces in (a) $S_{II} - I_1$; and (b) deviatoric stress space [34].

2.1.2. Isotropic plastic mechanism

The flow rule of isotropic part has been given by:

$$\dot{\varepsilon}^{pi}_{ij} = \lambda^i \frac{\partial f^i}{\partial \sigma_{ij}}, \tag{5}$$

in which f^i denotes the yield surface of the isotropic plastic mechanism. This surface is a perpendicular plane to the hydrostatic axis in the stress space as (Figure 1):

$$f^i(I_1, Q) = \frac{I_1}{3} - (Q + \frac{I_{1c}}{3}) \leq 0. \tag{6}$$

The hardening law is given by:

$$\dot{Q} = K_p \dot{q} = K_0^p \left(\frac{Q}{P_a}\right)^n \dot{q}, \tag{7}$$

where $\dot{q} = -\lambda^i \frac{\partial f^i}{\partial Q} = \lambda^i = \dot{\varepsilon}^{pi}_v$, K_0^p is a parameter of the model, and λ^i is the plastic multiplier associated to the isotropic plastic mechanism.

2.1.3. Deviatoric plastic mechanism

The yield surface of the deviatoric mechanism is expressed by the equation:

$$f^d(\sigma_{ij}, R) = S_{II} h(\theta) - R(I_1 + I_{1c}) \leq 0, \tag{8}$$

with $S_{II} = \sqrt{S_{ij}S_{ij}}$, $S_{ij} = \sigma_{ij} - \frac{\sigma_{kk}}{3}\delta_{ij}$, $I_1 = \sigma_{kk}$ and $h(\theta) = (1 - \gamma \cos 3\theta)^{1/6}$.

In the above equation, θ is the angle of Lode in S_i axes, R is the hardening parameter that characterizes the limit of elastic domain, γ is a constant parameter that defines the asymmetric form of the yield surface, and I_{1c} is a constant parameter for considering material cohesion. Figure 1 presents a diagram of the yield surface in the deviatoric plane.

Evolution of R is governed by an isotropic hardening law as:

$$R = \frac{AR_m r}{R_m + Ar}, \tag{9}$$

where A and R_m are two constant parameters and r is hardening variable which is obtained by normality law:

$$\dot{r} = -\lambda \frac{\partial f}{\partial R} = \lambda(I_1 + I_{1c})\xi. \tag{10}$$

According to Eq. (9), R_m is maximum value of R that characterizes failure state of material. With this parameter, the failure surface of model can be defined as $f^{dr}(\sigma_{ij}, R) = s_{II} h(\theta) - R_m(I_1 + I_{1c}) = 0$.

To consider the effect of confining stress on soil behavior, ξ has been introduced with the form:

$$\xi = \left(\frac{I_1}{3P_a}\right)^{-1.5}. \tag{11}$$

The flow rule for the deviatoric plastic mechanism is non-associated as:

$$\dot{\varepsilon}^{dp}_{ij} = \lambda^d G_{ij}, \tag{12}$$

where G_{ij} is the derivative of plastic potential function:

$$G_{ij} = \frac{\partial f^d}{\partial \sigma_{ij}} - \left(\frac{\partial f^d}{\partial \sigma_{kl}} n_{kl}\right) n_{ij}. \tag{13}$$

Here, n_{ij} is the tangent tensor to the plastic potential that is obtained from kinematic condition of $\dot{\varepsilon}^{dp}_{ij} n_{ij} = 0$, and the contractancy-dilatancy ($\dot{\varepsilon}^{dp}_v = \beta\left(\frac{S_{II}}{S^c_{II}} - 1\right)\frac{|S_{ij}\dot{e}^{dp}_{ij}|}{S_{II}}$) criteria of the model:

$$n_{ij} = \frac{\beta' \frac{S_{ij}}{S_{II}} - \delta_{ij}}{\sqrt{\beta'^2 + 3}}, \tag{14}$$

$$\text{with} \quad \beta' = \beta\left(\frac{S_{II}}{S^c_{II}} - 1\right) \operatorname{sign}(S_{ij}\dot{e}^{dp}_{ij}). \tag{15}$$

In the above equation, β is a parameter of the model and S^C_{II} represents the characteristic stress state that separates the contractancy and dilatancy states in the stress space. We can then define characteristic surface in the stress space, with an identical form to the failure surface (Figure 1):

$$f^c = S_{II}h(\theta) - R_c(I_1 + I_{1c}) = 0. \tag{16}$$

R_c is a parameter of the model that represents the average radius of this surface.

2.1.4. Viscoplastic part

Viscous formulation, similar to the elastoplastic part (basic model), has been decomposed into two parts: deviatoric and isotropic:

$$\dot{\varepsilon}_{ij}^{vp} = \eta\langle\Phi_1(F_1)\rangle G_{ij}^{vp} + \frac{\eta_i}{3}\langle\Phi_2(F_2)\rangle\delta_{ij}, \tag{17}$$

in which η is viscosity parameter of model, and $\Phi_1(F_1)$ is the function of overstress related to deviatoric loading:

$$\Phi_1(F_1) = \exp(N(R - R_v)) - 1. \tag{18}$$

N is one of the model parameters that design intensity of viscous deformation, and R is the mean radius of yield surface that is calculated using Eq. (8) as:

$$R = \frac{S_{II}h(\theta)}{I_1 + I_{1c}}. \tag{19}$$

Here, we define R_v as the hardening parameter in devatoric viscoplastic mechanism that depends on distance between current stress state and viscous state, history and properties of material, with the following expression:

$$\dot{R}_v = h\rho\Phi_1(F_1). \tag{20}$$

The history and properties of material is considered by h, defined as:

$$h = A_v I_1 \xi, \tag{21}$$

in which A_v is a constant parameter depending on soil type. ρ has been also defined for modeling the secondary creep phase as:

$$\rho = 1 - \omega\frac{R_v}{R_m}. \tag{22}$$

For $\omega = 1$, at the end of primary phase of creep, $\dot{R}_v$ and $R - R_v$ are equal to zero, therefore viscous deformation evolution is stopped. In the case of $\omega > 1$, at the certain time, ρ takes on a zero value. This means that the evolution of R_v is stopped, however, $R - R_v$ will take on a non-zero value resulting in a viscous deformation with constant velocity. G_{ij}^{vp} is derivative of viscoplastic potential function. Its expression is similar to derivative of plastic potential function in the basic model, except that β in Eq. (15) has been replaced by β_v that controls the volumetric deformation intensity in viscoplastic mechanism.

The viscous evolution due to change in mean stress is taken into account, using the following equation for $\Phi_2(F_2)$:

$$\Phi_2(F_2) = \left(\frac{I_1}{3P_c} - 1\right)^2, \tag{23}$$

in which $P_c = P_{co}\exp(c\varepsilon_{kk}^{vp})$, P_{co} is the initial consolidation pressure, and is one of the model parameters.

2.2. Parameters identification

For the elastoplastic part, all of the parameters can be determined easily by using classical laboratory tests results. Procedure for calibrating the model parameters has been detailed in [34,36]. For the parameters of viscoplastic mechanism, it is necessary to perform some of creep or relaxation tests. The elastoplastic-viscoplastic model presented above has been implemented in FLAC code [37,38]. Figure 2 shows the simulation results of typical creep triaxial tests in which the role of viscoplastic mechanism parameters and their sensibilities on model response have been presented.

3. Brief representation of Towheed tunnel

Towheed tunnel project is a 3003 m urban underground structure situated in Tehran city. It comprises an adjacent twin tunnel structure, shared by a middle interface wall, and a set of piles. The height and width of each of tunnels for the passage of the vehicles are 5 and 11 m, respectively. In this study a section of Towheed tunnel at kilometer (1+917) is selected as a case study. Geometry and boundary of section have been shown in Figure 3. Due to shortage in experimental results, ground media is assumed to be homogenous. Soil is modeled in dry situation because water table does not exist in soil layers up to 80 meter depth from ground surface. According to geotechnical studies report, some of mechanical parameters of ground material are presented in Table 1.

4. Model calibration using back analysis procedure

Using mechanical parameters of soil presented in Table 1, we obtained a primary estimation for different parameters of basic model. Then, model parameters were adjusted by application of back analysis process, presented in the following sections and regarding the field data for the selected part of tunnel.

4.1. Boundary conditions

According to Figure 4, a free displacement boundary condition was adopted at the ground surface. Neither horizontal nor vertical displacement takes place at the lower boundary because of hard bed layer existence with high density and SPT number (SPT higher than

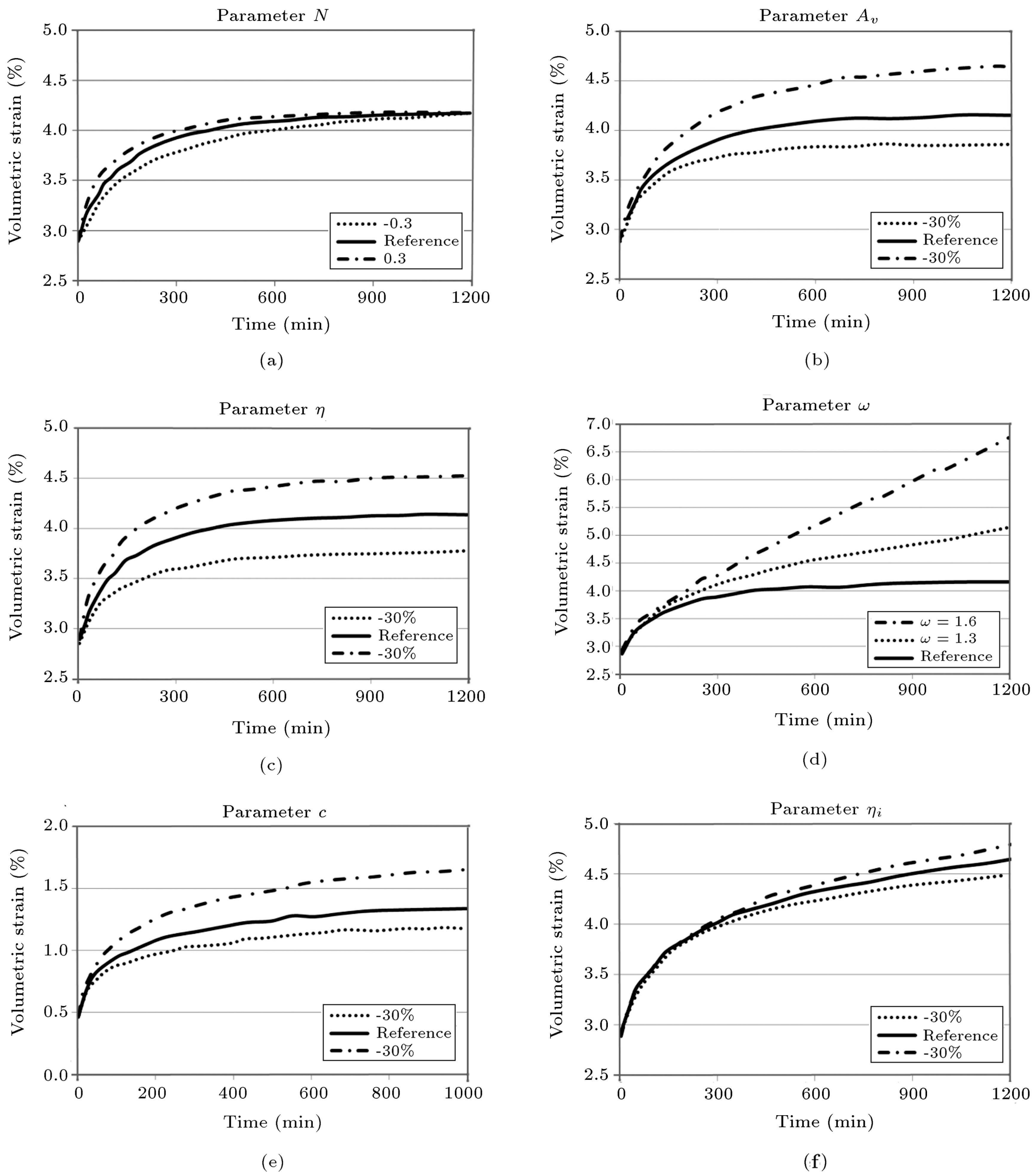

Figure 2. Creep triaxial tests simulation indicating the role of viscoplastic parameters on model response [34].

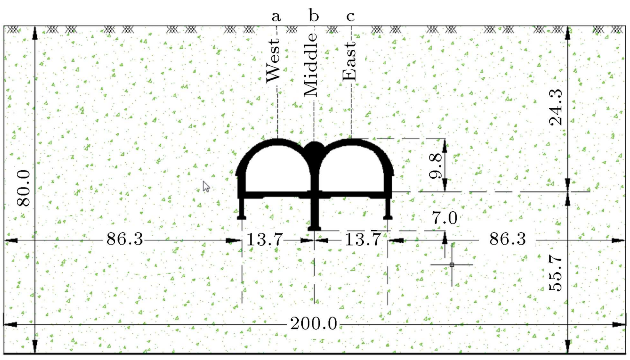

Figure 3. Towheed tunnel position (all sizes in meter). a, b and c are positions of in situ ground surface settlement measurements.

Table 1. Soil mechanical parameters.

SPT number	Cohesion (kPa)	Internal friction angle	γ (soil density) $(\frac{kN}{m^3})$
> 60	$c' = 42$	$\varphi' = 33°$	$18 - 19$

60 [39]). The lateral displacements at left and right hand boundary are both fixed as zero, but vertical displacement is free to be done. To choose the boundary dimension, there was a series of tunnel simulation was carried out by various vertical boundaries from center line. Based on obtained results, the value of 100 meters gives a good answer; so it was used for this study.

Table 2. Tunnel segments parameters.

	Steel middle column	Injection (grouting)	Lining	Shotcrete
Yong modulus E (kN/m^2)	2×10^{10}	6×10^7	6.8×10^7	3×10^7
Thickness or height of section (m)	0.3	0.4-0.5	0.7	0.3
ρ (kgf/m^3)	7800	1800	2300-2400	1800-2000

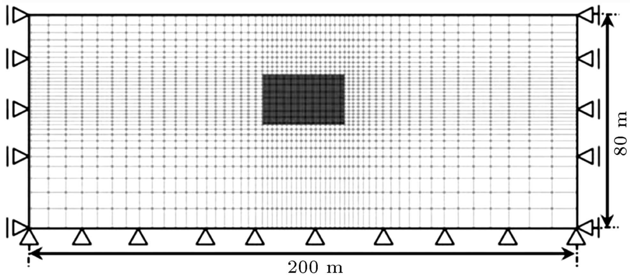

Figure 4. FDM mesh in numerical simulation.

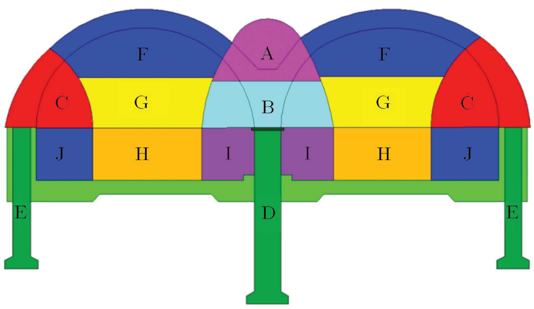

Figure 5. Excavation pattern of Towheed twin tunnels.

Therefore, the problem boundary is 200 m in width and 80 m in height.

4.2. Numerical analysis process

Finite difference analyses were carried out using the FLAC 2D [40]. Figure 5 shows the excavation pattern. As can be seen from this figure, the tunnel excavation begins from crown middle of tunnels (stages A and B); then, two left and right galleries are excavated (stage C). In this step, lining of C is done. These gallery are excavated for all the tunnel length which during the excavation of these three galleries piles are excavated and installed (stages D and E). After that, tunnel's crown (stage F) is excavated, and the steel beams are installed as a pilot longitudinal support for controlling tunnel's crown movements. Finally, in the excavation of stage G, the support steel column is placed on tunnel invert, and wall and crown lining of tunnels are performed. Then, stages H to J are excavated consecutively. Finally, lining of tunnels invert is performed. Tunnel lining parameters are listed in Table 2.

4.3. Sequential excavation simulation

Different steps in selected excavation pattern have been performed at different times during the advancement

Table 3. Stress release parameter in various tunneling procedures.

Excavation procedures	λ_d
Excavation without support	0.2-0.4
Excavation with shotcrete	0.5-0.6
Excavation with lining	1.0

of the tunnel face. In the numerical analysis process, for excavation of each region of tunnel face, the convergence-confinement method was applied [41]. In this method, the effects of 3D behavior on tunnel simulation in 2D analysis can be relatively taken into account. On the other hand, stress relaxation of tunnel face in numerical analysis can be simulated based on the relation between the closures of the unsupported tunnel and the distance from the face. Tunnel closure can also be related to traction forces acting on the tunnel periphery via a ground reaction curve. Thus, the tunnel relaxation as a function of the distance to the face can be specified in terms of tractions defined by a ground reaction curve and an expression relating closure to distance from the face. In this method, firstly, numerical analysis is done by obtaining nodal stresses on excavated surfaces. After that, soil elements are omitted, and the obtained stress will be applied to excavated faces in the inverse direction. It should be noted that, the excavation method of Towheed tunnel is principally based on NATM. Tunnel excavation pattern and divers stages (zones) of excavation have been presented in Figure 5. In each stage, firstly excavation is done using drum cutter, and afterward shotcrete is performed as an initial supporting system. Finally, lining is realized as cast in place method. Distance between tunnel face and shotcrete region is about 1-1.5 m and stress release scalar parameter is 0.2-0.4 in this step. For the region with shotcrete, stress release parameter has been considered between 0.5-0.6. Lining has been performed in the distance about 20-50 m away from excavation face. For this step, stress release parameter takes the maximum of its value, i.e. 1.0. The stress release parameter in various stages of excavation, installation of shotcrete and lining are listed in Table 3.

Ground surface settlements of tunnel in three different points (east, middle and west sides of tunnel) based on in situ measurements are shown in Figure 6. Because of the same surface settlements in east and west parts of tunnels, one of them is presented here.

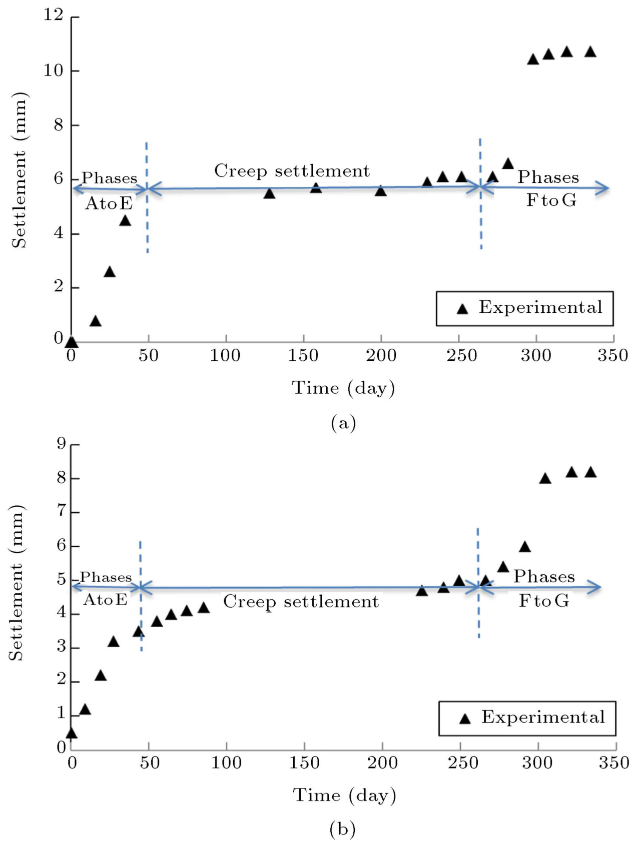

Figure 6. In situ time dependent settlement of ground surface: (a) Middle tunnels; and (b) east (= west) part of tunnel.

Table 4. Viscoplastic parameters of constitutive model.

$A_v = 0.006$ mPa^{-1}	$n = 0.25$	$\eta = 0.00011$ min^{-1}
$\omega = 1.4$		$\beta_v = -1.9$

4.4. Viscoplastic mechanism parameters

For viscoplastic part parameters, based on the simulation of creep test in triaxial condition and processing parameter sensitivity analysis and divers properties of ground, initial estimation has been assessed. The optimized parameters of viscoplastic mechanism are determined using the field results between E and F phases. In this stage, no excavation is done. On the other hand, total displacements are only because of time dependent deformation not due to tunnel excavation (construction phase). Iterative procedures are used to investigate these parameters. After each step of back analysis processes, the modified parameters are carried out by using these curves. Algorithm of iterative processes is shown in Figure 7. These processes are continued until differences of two subsequent displacements are about zero. The fitted curves of numerical and experimental data are shown in Figure 8, and the obtained parameters are listed in Table 4.

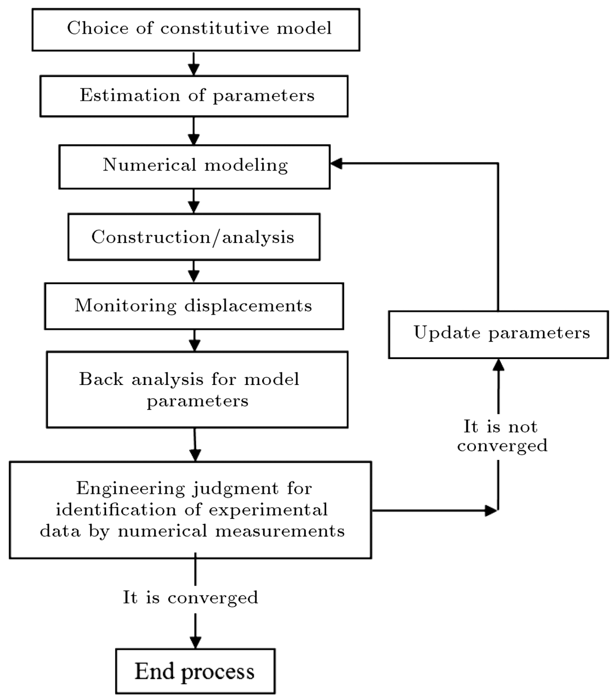

Figure 7. Different parts of one stage in back analysis used in this study.

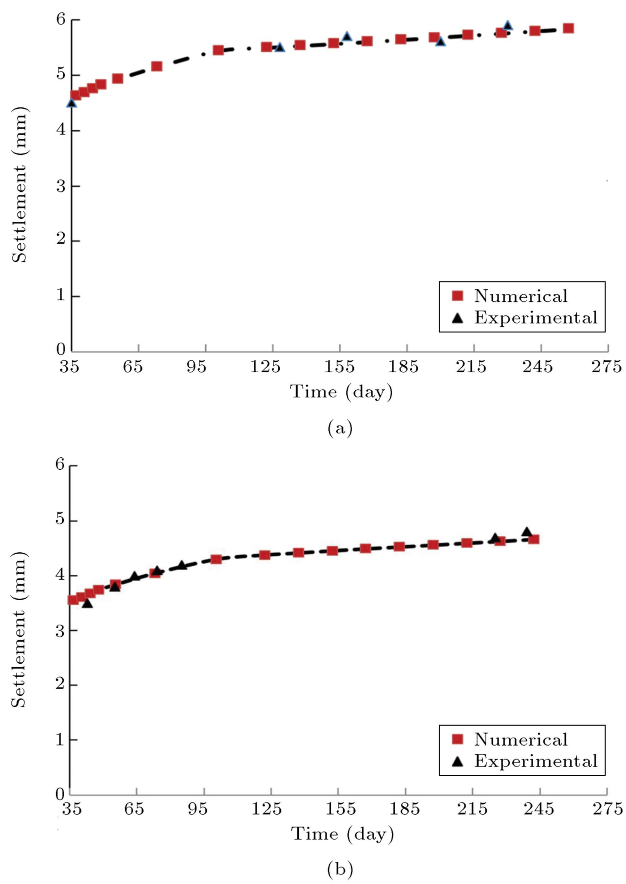

Figure 8. Calibarion curves of viscoplastic model parameters: (a) Middle tunnels; and (b) east (west) part of tunnel.

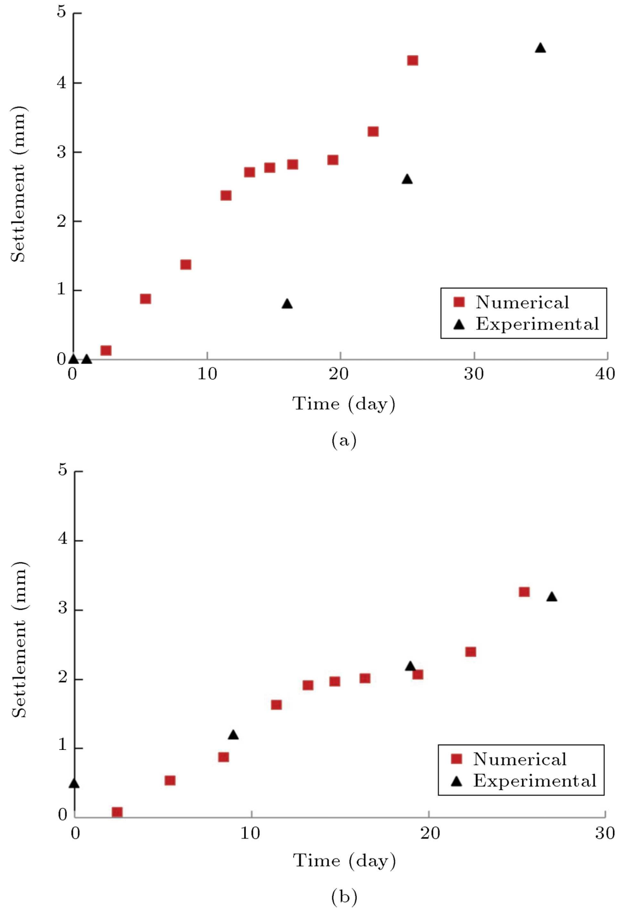

Figure 9. Calibarion curves of elastoplastic model parameters: (a) Middle tunnels; and (b) east (west) part of tunnel.

Table 5. Parameters of basic model.

Rc $= 0.277$	$\gamma = 0.85$	$I_{1c} = 1235$ kPa	$\beta = -1.0$
$n = 0.5$	$A = 0.5$ kPa^{-1}	$G_0 = 200$ MPa	$R_m = 0.355$
$K_0^e = 350$ MPa		$K_0^p = 600$ MPa	

4.5. Elastoplastic mechanism parameters

Elastoplastic parameters were firstly estimated based on mechanical parameters presented in Table 1. Then, using the same iterative process, these parameters were justified by conformity on field data in construction phase (Figure 7). The fitted curves of numerical and measurement data are shown in Figure 9. The values of parameters are listed in Table 5.

5. Safety evaluation of tunnel

In this section, with the obtained model parameters, a set of numerical analyses were performed for evaluating tunnel safety during and after construction.

5.1. Safety criteria definition

Two typical criteria for safety evaluation exist in literature one of which uses stress parameters and the other is based on deformation. Safety factor in stress criteria is obtained by comparing current stress state with yield or failure stress state. Yield criteria are most utilized in these cases. In the elastic-perfectly plastic constitutive models, yield surfaces are coincided to failure surface, so failure criterion is used for comparison. The Coulomb criterion, $\tau = \sigma \tan\varphi + c$, is more interesting for this case. On one hand, in elastoplastic constitutive models with hardening mechanism, yield criteria are different from those of failure surfaces. On the other hand, based on hardening mechanism, yield surface will be matched to failure surface in loading processes, so the yield criterion is a loading function characterized by current stress state. Therefore, safety evaluation can be attained using hardening stress parameters at the current and failure states.

In this work, tunnel safety is evaluated in two different ways corresponding to instantaneous (during excavation) and time-dependent (after excavation) behaviors, respectively. For excavation phase, hardening parameter of R in constitutive model can be used. This parameter defines the mean radius of yield surface, and its limit R_m designs the position of failure surface (Figure 1). By using equations of yield and failure surfaces, the values of R and R_m can be determined by the expressions:

$$R = \frac{S_{II} h(\theta)}{I_1 + I_{1c}}, \tag{24}$$

$$R_m = \frac{S_{II_{\text{Failure}}} h(\theta)_{\text{Failure}}}{I_{1\text{Failure}} + I_{1c}}. \tag{25}$$

The safety parameter can be defined now by:

$$F_1 = \frac{R_m}{R}. \tag{26}$$

The safety parameter mentioned above is not suitable for evaluating the tunnel safety during the time. Because the hardening parameter, R, that has stress nature may remain unchangeable in time. This is the case of creep deformation which occurs under a constant loading or unloading. For this reason, the good parameter for evaluating the tunnel safety is deformation. Although, the constitutive model cannot describe the third phase of creep (creep rupture), the capacity of model in generating secondary phase of creep (deformation with constant velocity) allows us to define a certain level of shear deformation ($\gamma_{\lim}$) corresponding to failure of material. Definition of shear strain in plane strain state is given as:

$$\gamma = \frac{1}{2}\left((\varepsilon_{xx} - \varepsilon_{yy})^2 + 4\varepsilon_{xy}^2\right)^{1/2}. \tag{27}$$

This limit shear deformation can be approximately estimated from experimental test result. In the case of classical triaxial test, shear strain is defined as $\gamma = \frac{1}{2}(\varepsilon_1 - \varepsilon_3)$. In this study, using results of drained triaxial test simulation, axial and volumetric strain corresponding to limit state were -0.9% and -0.3%, respectively. By application of relation $\varepsilon_v = \varepsilon_1 + 2\varepsilon_3$, limit shear strain will be equal to 0.6%. Therefore, the comparison of actual shear strain during the time with the limit shear strain presents level of safety existing in each point of tunnel media. The safety factor in this case can be defined by:

$$F_2 = \frac{\gamma_{\lim}}{\gamma}. \tag{28}$$

6. Results of analyses

The numerical analysis of the Towheed tunnel are executed for three different stages (stage E related to three trial galleries excavation, stage G relevant to completion of top heading of tunnel and J is pertinent to end of tunnel excavation) according to Figure 5. Results of tunnel analyses and distribution of zones and time-dependent safety factor (F_1) contours are shown in Figure 10(a), (b) and (c), respectively. The reader should note the difference in the extent of these zones and the magnitude of the generated displacements in each stage. Stage E is compared with two other stages G and J, and safety numbers have been drastically increased by increasing values of F_1. A comparison of stages G and J reveals that stage G has a safer behavior related to larger values of F_1. As shown in this figure, safety number is reduced with increase of tunnel opening region. Crown in stages of G and J is safer comparing to other parts of tunnel face, such as tunnel walls and invert. However, according to the results of analyses, in different stages, safety contours develop all over the tunnel section, including the crown, sidewalls and the invert. In addition, the calculated safety numbers in invert are significantly less than other parts of tunnel.

The distributions of shear strain in percent for instantaneous cases (stages G and H) are plotted in Figure 11. As can be seen from Figure 11(c), the instantaneous safety factor in crown of tunnel has the closest value ($F_2 = 1.5$) to limit deformation. In this case, it is essential to use in situ instruments, such as tunnel convergence, and ground surface settlement to control the serviceability of tunnel in this stage. It should be noted that, the minimum values of F_1 and F_2 are in a same situation (Figure 10(c)).

To take the effect of time on tunnel safety, distribution of F_2 is calculated for 200 days after tunnel excavation. The results of analyses are shown in Figure 12. As can be seen from Figure 12(a), time has a significant effect on tunnel behavior. In each stage, time parameter (200 days) induces to increase shear strain about 1.25-folds in comparison with in-

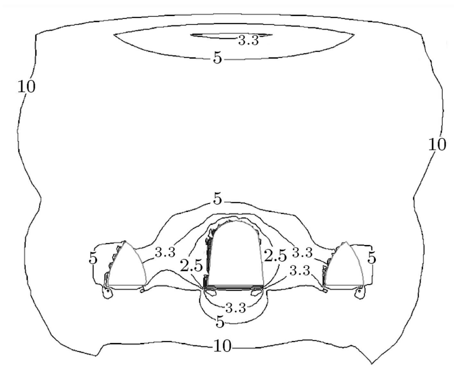

(a)

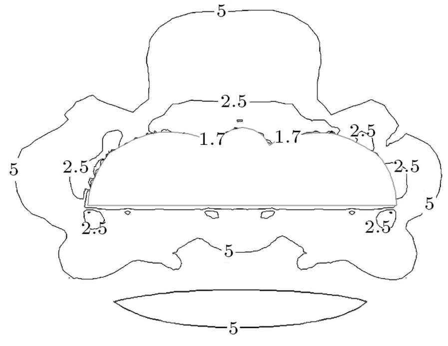

(b)

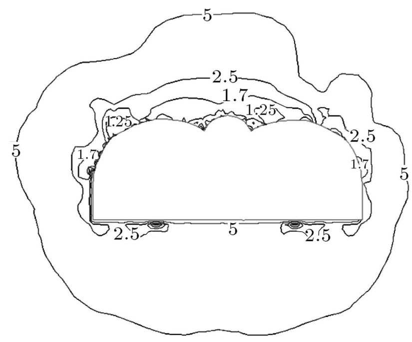

(c)

Figure 10. Contours of F_1 during excavation in different stages: (a) Stage E; (b) stage G; and (c) stage J.

stantaneous values. These differences in instantaneous and time-dependent values mainly exist near the tunnel excavation face and are decreased by being away from regions near the tunnel. If stage G delaying about 200 days after top heading complete excavation is considered, it will generate critical values of shear strain in tunnels crown (Figure 12(b)). This means that tunnel needs extra support system in this case. However Towheed tunnel was excavated without any important time delay.

7. Conclusions

The following conclusions can be drawn from this study:

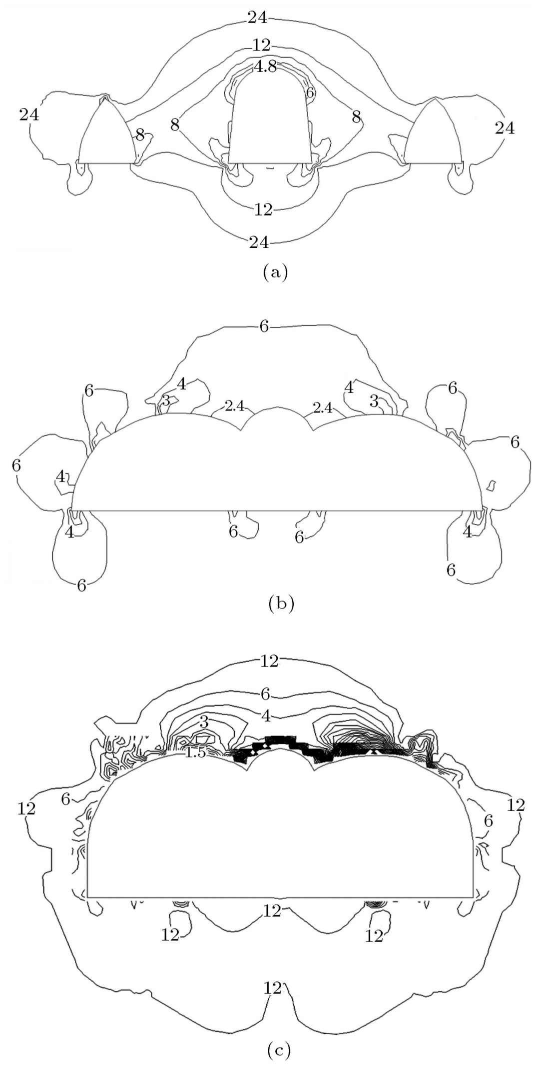

Figure 11. Contours of F_2 during excavation in different stages: (a) Stage E; (b) stage G; and (c) stage J.

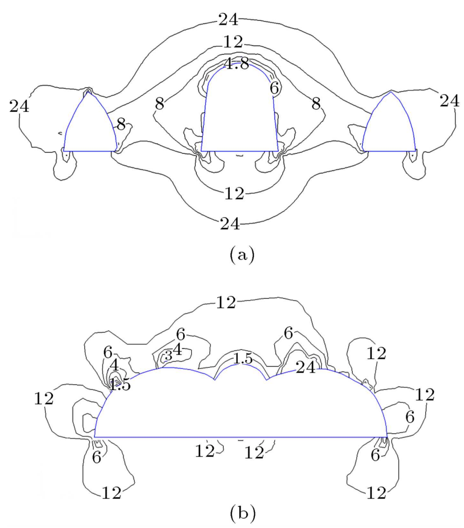

Figure 12. Contours of F_2 around tunnel in different stages, 200 days after excavation: (a) Stage E; and (b) stage G.

1. To describe time-dependent behavior of geomaterials, it is necessary to implement the appropriate constitutive models in the calculation codes. In this regard, elastoplastic-viscoplastic constitutive models are in priority.

2. As a result, the used constitutive model in this study is characterized by the following features: (1) Being capable of describing plastic state for instantaneous loadings regardless of compression or dilation and failure; (2) Being useful in generation of the time-dependent deformations (primary and secondary creeps, relaxation and rate effects); (3) The hardening parameter R provides a clear index for describing material states (elastic, plastic or failure). Comparison of R with its maximum value, R_m defines also a simple expression for safety factor.

3. The result of back analysis shows a good capacity of constitutive model in reproduction of the short-term and the long-term deformations of Towheed tunnel in different excavation processes and various soil and tunnel conditions. Capacity of constitutive model in describing the secondary creep phase allowed us to study the evolution of deformation with constant velocity during the time. In comparison with limit deformation, the failure of material due to creep can be estimated.

4. According to the obtained results, tunnel crown has a lower safety than the other part of faces, both in short and long term simulations. With this study, we can globally conclude that construction stages of Towheed tunnel have been done under safe conditions. These safe conditions can be generalized as a prediction also for life time of tunnel.

References

1. Abd El Salam, M.E. "Historic nile crossing by a bored tunnel", *Tunn. Undergr. Sp. Tech.*, **14**(3), pp. 257-265 (1999).

2. Bernat, S. and Cambou, B. "Soil-structure interaction in shield tunneling in soft soil", *Computers and Geotechnics*, **22**, pp. 221-242 (1998).

3. Bobet, A. and Einstein, H.H. "Tunnel reinforcement with rockbolts", *Tunn. Undergr. Sp. Tech.*, **26**, pp. 100-123 (2011).

4. Bobet, B., Atistorenas, G. and Einstein, H. "Feasibility analysis for a radioactive waste repository tunnel", *Tunn. Undergr. Sp. Tech.*, **13**(4), pp. 409-426 (1999).

5. Carranza-Torres, C. and Fairhurst, C. "Application of the convergence-confinement method of tunnel design to rock masses that satisfy the hoek-brown failure criterion", *Tunn. Undergr. Sp. Tech.*, **15**(2), pp. 187-213 (2000).

6. Desari, G.R., Rawlings, C.G. and Bolton, M.D. "Numerical modelling of a NATM tunnel construction in London clay", *Proc. of the International Symp. on Geotech. Aspects of Underg. Const. in Soft Ground.*, pp. 491-496 (1996).

7. Guan, Z., Jiang, Y. and Tanabasi, Y. "Ground reaction analyses in conventional tunnelling excavation", *Tunn. Undergr. Sp. Tech.*, **22**, pp. 230-237 (2007).

8. Jao, M. and Wang, M.C. "Stability of strip footings above concrete-lined soft ground tunnels", *Tunn. Undergr. Sp. Tech.*, **13**(4), pp. 427-434 (1998).

9. Jeon, J.S., Martin, C.D., Chan, D.H. and Kim, J.S. "Predicting ground conditions ahead of the tunnel face by vector orientation analysis", *Tunn. Undergr. Sp. Tech.*, **20**, pp. 344-355 (2005).

10. Kasper, T. and Meschke, G. "On the influence of face pressure, grouting pressure and TBM design in soft ground tunneling", *Tunn. Undergr. Sp. Tech.*, **21**, pp. 160-171 (2006).

11. Kirzhner, F. and Rosenhouse, G. "Numerical analysis of tunnel dynamic response to earth motions", *Tunn. Undergr. Sp. Tech.*, **15**(3), pp. 249-258 (2000).

12. Potts, D.M. and Zdravkovic, L. "Finite element analysis in geotechnical engineering: Application", **2**, Thomas Telford, London (2001).

13. Potts, D.M. and Zdravkovic, L. "Finite element analysis in geotechnical engineering", *Theory*, **1**, Thomas Telford, London (1999).

14. Yoo, C. and Shin, H.K. "Deformation behaviour of tunnel face reinforced with longitudinal pipes - laboratory and numerical investigation", *Tunn. Undergr. Sp. Tech.*, **18**, pp. 303-319 (2003).

15. Augustesen, A., Liingaard, M. and Lade, P.V. "Examination of models for time dependent behavior of soils", *15th ASCE Eng. Mech. Conf.*, Columbia University (2002).

16. Kontogianni, V. and Stiros, S. "Induced deformation during tunnel excavation: Evidence from geodetic monitoring", *Eng. Geology.*, **79**(1-2), pp. 115-126 (2005).

17. Kontogianni, V., Psimoulis, P. and Stiros, S. "What is the contribution of time-dependent deformation in tunnel convergence?", *Eng. Geol.*, **82**, pp. 264-267 (2006).

18. Shalabi, F.I. "FE analysis of time-dependent behavior of tunneling in squeezing ground using two different creep models", *Tunn. Undergr. Sp. Tech.*, **20**, pp. 271-279 (2005).

19. Perzyna, P. "Fundamental problems in viscoplasticity", *Adv. in Appl. Mech.*, **9**, pp. 243-277 (1966).

20. Adachi, T., Oka, F. and Mimura, M. "Mathematical structure of an overstress elasto-viscoplastic model for clay", *Soil. and Found.*, **22**(3), pp. 57-70 (1987).

21. Dafalias, Y. "Bounding surface elastoplasticity-viscoplasticity for particulate cohesive media", *Proc. of the IUTAM Symp. on Defor. and Failure of Gran. Materials*, pp. 97-107 (1982).

22. Dragon, A. and Mroz, Z. "A model for creep plastic creep of rock-like materials accounting for the kinetics of fracture", *In. J. of Rock Mech. and Min. Sci. Geom.*, **16**, pp. 253-259 (1979).

23. Katona, M.G. "Evaluation of viscoplastic cap model", *Geotech. Eng. ASCE.*, **110**(8), pp. 1106-1125 (1984).

24. Matsui, T. and Abe, N. "Elasto-viscoplastic constitutive equation of normally consolidated clay based on flow surface theory", *Proceedings of the 5th ICONMG*, pp. 407-413 (1985).

25. Nova, R. "A viscoplastic constitutive model for normally consolidated clay", *Proc. of the IUTAM Sym. on Deformation and Failure of Granular Materials*, pp. 287-295 (1982).

26. Sekiguchi, H. "Theory of undrained creep rupture of normally consolidated clay based on elasto-viscoplasticity", *Soils and Found.*, **24**(1), pp. 129-147 (1984).

27. Oka, F. "A cyclic elasto-viscoplastic constitutive model based on nonlinear hardening rule", *Proc. of the 4th Inter. Symp. on Numerical Models in Geomech.*, Balkema., **1**, pp. 105-114 (1992).

28. Kim, Y.S. "Dynamic behavior characteristics of clay in wide strain range based on viscoelastic-viscoplastic constitutive model", *Inter. J. of Offsh. and Polar Eng.*, **16**(2), pp. 153-160 (2006).

29. Kaliakin, N. and Dafalias, F. "Theoretical aspects of the elastoplastic-viscoplastic bounding surface model for cohesive soils", *Soils and Found.*, **30**(3), pp. 11-24 (1990).

30. Sandrone, F. and Labiouse, V. "Identification and analysis of Swiss national road tunnels pathologies", *Tunn. Undergr. Sp. Tech.*, **26**, pp. 374-390 (2011).

31. Anagnostou, G. and Kovari, K. "Face stability conditions with earth-pressure-balanced shields", *Tunn. Undergr. Sp. Tech.*, **11**(2), pp. 165-173 (1996).

32. Atkinson, J.H. and Mair, R.J. "Soil mechanics aspects of soft ground tunnelling", *Gro. Eng.*, **14**(5), pp. 20-38 (1981).

33. Rangel, J.L., Iturrarán-Viveros, U., Gustavo Ayala, A. and Cervantes, F. "Tunnel stability analysis during construction using a neuro-fuzzy system", *Int. J. Numer. Anal. Meth. Geomech.*, **29**, pp. 1433-1456 (2005).

34. Maleki, M. "An elastoplastic-viscoplastic constitutive model for soils", *Sharif J. of Sci. and Tech.*, **2-26**(2), pp. 29-38 (2009).

35. Cambou, B. and Jafari, K. "Constitutive model for cohesionless soils", [Modèle de comportement des sols non cohérents], *Revue Francaise de Géotechnique.*, **44**, pp. 43-55 (1988).

36. Maleki, M. "Hierarchical modeling of soils behavior", [Modélisation hierarchisée du comportment des sols], PhD. Thesis, Ecole Centrale de Lyon, France (1998).

37. Maleki, M., Cambou, B. and Dubujet, Ph. "Hierarchical modeling of soils behavior", *European Journal of Environmental and Civil Engineering*, **4**, pp. 895-928 (2000).

38. Maleki, M. and Mirzaie, S. "Implemention of an elastoplastic-viscoplastic constitutive model in FLAC code and its application on prediction of unsupported excavation behavior", *5th National Cong. on Civil Eng.*, Mashhad, Iran (2010).

39. Mousivand, M. "Application of an elastoplastic-viscoplastic constitutive model for time-dependent behavior of tunnel in soft ground", Msc. Theses, Bu Ali Sina Universtiy, Hamedan, Iran, 150 p (2011).

40. Itasca Consulting Group, Inc. "Fast lagrangian analysis of continua", *FLAC Manual* (2002).

41. Panet, M. and Guenot, A. "Analysis of convergence behind the face of a tunnel", *Tunnelling 82. IMM*, London, pp. 197-204 (1982).

Biographies

Mohammad Maleki received the PhD degree in Civil Engineering from the Ecole Centrale de Lyon (France). Currently he is an associate professor in the faculty of engineering at Bu-Ali Sina University. His research interests include constitutive modelling of geomaterials, validation of calculation codes in geotechnical engineering and identification of constitutive model parameters.

Mohsen Mousivand is a PhD student in the Department of Civil Engineering at Islamic Azad University, Science and Research Branch, Tehran, Iran. He received his MSc from the University of Bu Ali Sina, Hamedan, Iran. And also has BS graduate in civil engineering from Islamic Azad University, Karaj Branch, Karaj, Alborz, Iran. His research interests are in the field of numerical and analytical methods in geomechanics. He has worked extensively on the analysis and application of elasto-plastic finite element programs to the analysis of real geotechnical structures. His additional experience includes design of an underground structure and surface excavations.